

DEM REGISTRATION, ALIGNMENT AND EVALUATION FOR SAR INTERFEROMETRY

Zhengxiao Li ^a, James Bethel ^b

^a ERDAS, Inc. (Leica Geosystems Geospatial Imaging), 5051 Peachtree Corners Circle, Norcross, Georgia 30092, USA
– tonybest@gmail.com

^b Purdue University, School of Civil Engineering, 550 Stadium Mall Drive, West Lafayette, IN 47907-2051, USA –
bethel@purdue.edu

KEY WORDS: DEM, Accuracy assessment, SAR Interferometry, Digital elevation models, Registration, Image matching, Transformation, Parameters

ABSTRACT:

To generate an accurate digital elevation model (DEM), Interferometric Synthetic Aperture Radar (InSAR) requires precise orbit data and baseline information, which are not always available. An alternative approach is to apply quality ground control points (GCPs) into the InSAR processing. However, locating high quality GCPs can also be difficult task, due to the low spatial resolution and radiometric response of synthetic aperture radar (SAR) images. This paper presents a method to register and align an InSAR DEM, generated from SAR images without precise orbit or baseline information and without GCPs, to an existing coarse reference DEM for refinement. The results showed this method achieves a comparable or even better accuracy than applying GCPs into InSAR processing. It was also found that the existing DEM with lower resolution than the InSAR DEM could be a good reference for this registration and alignment, i.e. refinement. ERS1/2 tandem SAR image pairs were used for 16-meter (post spacing) InSAR DEM generation. Both InSAR processing with and without applying GCPs were conducted for comparison purposes. The InSAR DEM was registered and aligned to SRTM 3 Arc Second data, a global reference DEM. The “truth” DEM used for accuracy evaluation is a higher accuracy DEM from aerial imagery with post spacing of 1.5 meters and vertical accuracy of 1.8 meters.

1. INTRODUCTION

In order to generate an accurate digital elevation model (DEM) through Interferometric Synthetic Aperture Radar (InSAR) processing, by conventional methods, precise orbit and baseline data are required for processing. Unfortunately, these are not always available. An alternative approach is to apply ground control points (GCPs), which are used to adjust and refine orbit and baseline data (Zebker et al., 1994), or to refine the final InSAR DEM externally (Ge et al., 2004). However, due to the low spatial resolution and radiometric response of synthetic aperture radar (SAR) images, locating high quality GCPs can also be difficult task (Sowter et al., 2006; Toutin et al., 1998).

Another method was developed to refine an InSAR DEM that does not require precise orbit and baseline data or accurate GCPs. The approach involves registering and aligning the new InSAR DEM to an existing coarse reference DEM. No orbit or baseline adjustment is needed. Coverage, currency, or accuracy issues may prohibit direct use of these existing reference DEMs, but they may be good enough to align and register the InSAR DEM. They could also reduce the InSAR processed DEM errors caused by the lack of precise orbit and baseline knowledge, and lack of accurate GCPs.

Registration is also called marching, which is to search for corresponding control points on InSAR DEM and reference DEM. Those corresponding control points are then used for deriving seven-parameter transformation equations by least squares. Through the seven-parameter transformation equations, InSAR DEM is converted and aligned to reference DEM.

The results show that this method achieves a comparable or even better accuracy than incorporating GCPs into the InSAR

processing. It is also found that an existing DEM with lower spatial resolution than the InSAR DEM can be used as a reference for the registration and alignment, i.e. refinement.

In this research, two pairs of ERS1/2 tandem SAR images were used for 16-meter (post spacing) InSAR DEM generation. InSAR processing with and without applying GCPs was performed for comparison purposes. The InSAR DEM was registered and aligned to SRTM (Shuttle Radar Topography Mission) 3 Arc Second data, a global reference DEM. The “truth” DEM used for accuracy evaluation is a higher accuracy DEM from aerial imagery with post spacing of 1.5 meters and vertical accuracy of 1.8 meters.

2. METHODOLOGY AND ALGORITHM

Due to the inaccurate orbit and baseline information, the InSAR DEM distortion is mostly vertical tilt and offset, horizontal offset, and scaling or stretch. The approach of registration and alignment is to find the geometric relation between the newly developed InSAR DEM and the existing coarse DEM, and to correct the InSAR DEM. The existing coarse DEM may have the lower resolution, but it could be good to reduce the systematic bias error of the InSAR DEM with higher resolution, horizontally and vertically.

Conventional image registration can be envisioned as a 2.5 dimensional problem. Nearly aligned DEMs may also be handled as a 2.5 dimensional problem, whereas significant misalignments may require handling as a full three dimensional problem. A three dimensional (3D) model can be approached as a simultaneous solution or as a series of lower order

registrations and transformations which, taken together, are equivalent to a three dimensional solution.

There have been a number of studies on DEM matching and 3D surface matching. The robust estimation was used for detecting the change between surface models without the assistance of ground control points. (LI et al., 2001; Pilgrim, 1996) A “multimatch-mutimosaic” approach was used for matching and mosaicing TOPSAR DEM data. The cross-correlation was calculated to find the horizontal and vertical offsets. A number of offsets were then used to derive 3D affine transformation, through which the DEM data were converted and mosaiced together. (Lu et al., 2003) The most commonly applied approach for matching 3D point clouds is least squares registration. (Gruen and Akca, 2005) An approach fusing ASTER DEM and SRTM is similar to “multimatch-mutimosaic”. The conjugate points were selected through valley and ridge lines. Only vertical shift was applied for aligning the two DEMs. (Karkee et al., 2006)

In this study, the cross-correlation through frequency domain is applied for searching for 3D conjugate points on InSAR DEM and reference DEM. Those 3D control points are then used for deriving seven-parameter 3D transformation equations between InSAR DEM and reference DEM. After InSAR DEM is converted through the seven-parameter transformation equations, the resampling is needed to obtain the InSAR DEM with regular grids of posts.

The refined InSAR DEM is then evaluated against the truth DEM. The InSAR DEM with GCPs applied is also evaluated against the same truth DEM. The errors of those two InSAR DEMs are compared to each other.

2.1 InSAR DEM to reference DEM registration

Cross-correlation is the most commonly used approach for image registration. The algorithm is simple to implement, the speed and accuracy are acceptable, and it is not data sensitive and can be applied in automatic registration easily. The cross-correlation is used to search for conjugate points in InSAR DEM registration.

Cross-correlation can be calculated in the space domain as Eq. (1), where image patch A has dimensions (Ma, Na) and image patch B has dimensions (Mb, Nb) . $Conj$ is the complex conjugate. It has maximum $C(i, j)$ when two images are aligned with each other. (Orfanidis, 1996)

$$C(i, j) = \left| \sum_{m=0}^{Ma-1} \sum_{n=0}^{Na-1} A(m, n) \cdot conj(B(m+i, n+j)) \right| \quad (1)$$

$0 \leq i < Ma + Mb - 1 \quad \text{and} \quad 0 \leq j < Na + Nb - 1$

Cross-correlation can also be calculated in frequency domain. Convolution in the space domain can be performed as multiplication in the spatial frequency domain. Both image patches A and B are transformed into the frequency domain through two-dimensional (2D) Fourier transformation. Image patch A is then multiplied by complex conjugate of B or vice versa. The cross-correlation is computed by transforming the product back to the spatial domain. The peak of the modulus of the transformed product is the location of maximum cross-correlation (Eq. (2)). Cross-correlation in frequency domain is much faster than cross-correlation in the spatial domain.

$$C(i, j) = \left| F^{-1} \{ F \{ A \} \cdot F^* \{ B \} \} \right| \quad (2)$$

In this study, the cross-correlation in the frequency domain was calculated to find highly correlated conjugate points.

Not all maximum values of cross-correlation are used as correlation peaks to calculate offsets between conjugate points. First, a maximum-to-average ratio (the ratio of maximum cross-correlation to the average cross-correlation, or MAR (Eq. (3)) is computed. If the MAR is lower than certain threshold, this maximum value is not considered as correlation peak and this pair of conjugate points is not used.

$$MAR = \frac{Max\{C(i, j)\}}{Mean\{C(i, j)\}} \quad (3)$$

Second, if the offsets (i_{Cmax}, j_{Cmax}) between two conjugate points are much larger than other conjugate points, this peak will be considered as an outlier and is not included either.

2.2 Solving seven-parameter transformation equations

Seven-parameter transformation equations express the space relationship between two sets of 3D points, which are InSAR DEM posts and reference DEM posts. The seven parameters include one uniform scale, three rotations, and three translations (Eq. (4)). (x, y, h) are 3D coordinates of InSAR DEM posts, and (X, Y, H) are 3D coordinates of reference DEM posts or 3D coordinates of transformed InSAR DEM posts. S is the uniform scale, $\omega, \varphi,$ and κ are the rotation angles with regard to x, y and z axis. (tx, ty, tz) are the translations from rotated and scaled InSAR DEM to reference DEM. (Mikhail et al., 2001)

$$\begin{bmatrix} X \\ Y \\ H \end{bmatrix} = S \cdot \begin{bmatrix} \cos(\kappa) & \sin(\kappa) & 0 \\ -\sin(\kappa) & \cos(\kappa) & 0 \\ 0 & 0 & 1 \end{bmatrix} \begin{bmatrix} \cos(\varphi) & 0 & -\sin(\varphi) \\ 0 & 1 & 0 \\ \sin(\varphi) & 0 & \cos(\varphi) \end{bmatrix} \begin{bmatrix} 1 & 0 & 0 \\ 0 & \cos(\omega) & \sin(\omega) \\ 0 & -\sin(\omega) & \cos(\omega) \end{bmatrix} \begin{bmatrix} x \\ y \\ h \end{bmatrix} + \begin{bmatrix} tx \\ ty \\ tz \end{bmatrix} \quad (4)$$

A number of conjugate points are acquired through InSAR DEM to reference DEM registration. Those conjugate points are inserted into Eq. (4). A solution for the seven parameters is derived through the least squares approach.

2.3 Transforming and resampling InSAR DEM

The InSAR DEM is transformed through those seven-parameter transformation equations. However, the posts of the output InSAR DEM are not on the regular grids. A step of resampling is required to convert irregular InSAR DEM posts into regular posts.

2.4 InSAR DEM Evaluation

The root mean square error (RMSE, eq. (5)) is commonly used for InSAR DEM evaluation (Lin et al., 1994; Miliareisis and Paraschou, 2005; Rufino et al., 1996; Rufino et al., 1998; Zebker et al., 1994).

$$RMSE = \sqrt{\frac{e_1^2 + e_2^2 + \dots + e_n^2}{n}} \quad (5)$$

In eq. (5), e_i is the elevation difference between an InSAR DEM and a truth DEM and n is the number of points involved in the evaluation.

3. DATA, TOOLS AND EXPERIMENT

3.1 Data

The SAR data are two pairs of ERS-1/2 tandem mode single-look complex images. The first pair covers about 10 counties in northern Indiana, USA, where the terrain is relatively flat. The second pair covers about 10 counties in southern Indiana, USA, with more varied terrain. Both pairs were acquired in fall 1995 (Figure 1).



Figure 1 SAR images overlaying Indiana counties

The USGS SRTM 3 arc second DEM are used as the reference DEM for the InSAR DEM registration and alignment. It has global coverage between 60 degrees N and 56 degrees S latitude. The vertical accuracy is +/-10 meters RMSE. The post-spacing or GSD (ground sample distance) is about 90 meters. (Figure 2)

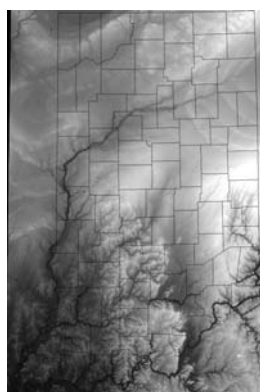


Figure 2 SRTM 3" DEM overlaying Indiana counties

The "truth DEM" was produced from the "Indiana 2005 Statewide Orthophotography Project", which includes both ortho imagery and a high resolution DEM (Orthophoto DEM). The DEM has 5-foot (~1.5m) post spacing and 6-foot (~1.8m) vertical accuracy at 95% confidence level. (Figure 3)

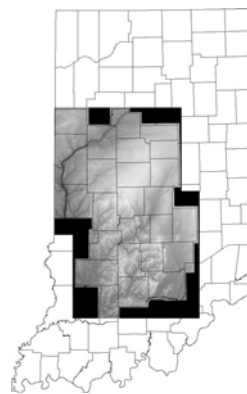


Figure 3 Orthophoto DEM overlaying Indiana counties

All of those DEMs, including processed InSAR DEM, are reprojected into WGS84 UTM (Zone 16 North) with post spacing of 16 meters, and the vertical datum of WGS84 ellipsoidal height in meter.

Selecting GCPs on SAR images proved to be difficult. GCPs maintained for optical imagery are not visible on ERS SAR images unless corner reflectors are placed during acquisition or the target and background are large and have quite different backscatter. In this study, GCPs are derived from a combination of ortho imagery for planimetry and the associated DEM for elevation, with features also visible on the SAR images.

3.2 Tools

(Leica) ERDAS IMAGINE was used for InSAR DEM processing. GCPs are applied in the processing for the second workflow.

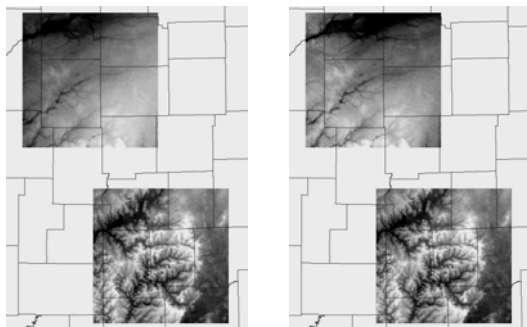
Matlab program was developed for the registration of InSAR DEM and reference DEM, searching for the conjugate points, transforming and resampling InSAR DEM, and InSAR DEM evaluation against "truth DEM".

C program from "Introduction to Modern Photogrammetry" was used for deriving seven-parameter transformation equations from 3D conjugate points. (Mikhail et al., 2001)

3.3 Experiment

In this study, the primary experiment was to compare the accuracy of the refined InSAR DEM with no GCPs applied in InSAR processing, to the accuracy of the GCP assisted InSAR DEM. Both were evaluated against the independent, high resolution DEM.

Two InSAR processes were performed for each InSAR pair: the first process had no GCPs applied and the second process had 10 GCPs applied. Figure 4 displays the subsets of InSAR DEM with and without GCPs applied.



a) 10 GCPs applied b) No GCPs applied

Figure 4 Subsets of InSAR DEM overlaying Indiana counties

Both InSAR DEMs (with and without GCPs applied) were then registered with reference DEM (SRTM). An example of the cross-correlation is illustrated in Figure 5.

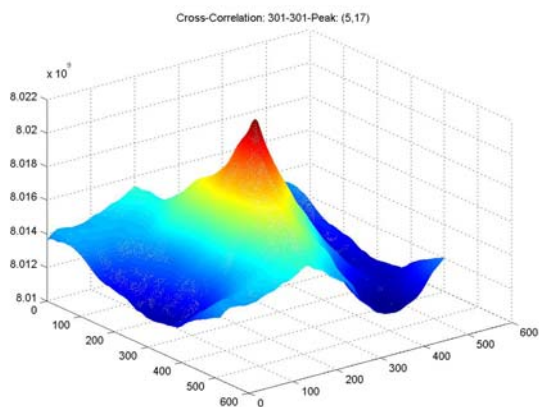


Figure 5 Cross-correlation of InSAR DEM and reference DEM

The peak location $(\Delta y, \Delta x) = (5, 17)$ is the horizontal offsets between one patch of InSAR DEM and one patch of reference DEM. The conjugate points are determined from the offsets: $(x, y) = (318, 306)$ and $(X, Y) = (301, 301)$, as $(x, y) - (X, Y) = (17, 5)$. Elevations h and H are then acquired through the location of conjugate points on InSAR DEM and reference DEM. The pattern of conjugate points is demonstrated in Figure 6.

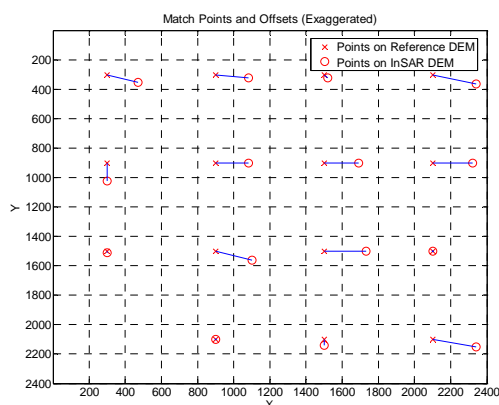


Figure 6 Pattern of conjugate points

Those conjugate points are listed in Table 1. The seven-parameter transformation equations were derived from those conjugate points through least squares approach.

Match Points	x	y	h (m)	X	Y	H (m)
1	318	306	173.777	301	301	175.494
2	919	303	142.618	901	301	154.377
...

Table 1 Conjugate points

The InSAR DEM was then transformed through the seven-parameter transformation equations and resampled into regular posts. RMSE of the new InSAR DEM was computed against the “truth DEM”.

4. RESULTS AND ANALYSIS

The results of RMSE are in Table 2.

Location (Average Slope)	Number of GCPs	RMSE Before Alignment (meter)	RMSE After Alignment (meter)
North (1.62°)	0	236.054	4.779
	10	12.477	4.085
South (4.13°)	0	117.954	12.421
	10	18.370	12.192

Table 2 RMSE of InSAR DEM against “Truth DEM”

GCPs applied INSAR processing yields much more accurate InSAR DEM than no GCPs applied, before any registration and alignment (12.477 m \ll 236.054 m and 18.370 m \ll 117.954 m).

After registration and alignment, the accuracy of refined InSAR DEM without GCPs applied improved tremendously, from 236.054 m to 4.779 m and from 117.954 m to 12.421 m. They are also much better than GCPs applied InSAR DEM without refinement, as 4.779 m $<$ 12.477 m and 12.421 m $<$ 18.370 m.

If applying both GCPs in the InSAR DEM processing and refinement in the post-InSAR DEM processing, the accuracy gets more improved, but not much over refinement alone: 4.085 m $<$ 4.779 m and 12.192 m $<$ 12.421 m.

The orbit data and terrain variation have different effects on InSAR DEM accuracy. Without GCPs applied or DEM refinement, the accuracy is mostly decided by the precision of orbit data, as both Indiana north and Indiana south have the huge InSAR DEM error (236.054 m and 117.954 m). After applying GCPs or refining InSAR DEM, the accuracy is related to the terrain variation. Indiana south has the larger error (18.370 m $>$ 12.477 m and 12.421 m $>$ 4.779 m), as it has the higher average slope (4.13 degrees $>$ 1.62 degrees)

5. CONCLUSION

Integrating GCPs into InSAR processing produces a final DEM with acceptable accuracy. InSAR DEM refinement substitutes DEM registration and alignment for applying imprecise orbit

and baseline information or locating indistinct ground control points (GCPs) in InSAR processing. If a reference DEM is available, registration and alignment can make an InSAR DEM with good accuracy, comparable to applying GCPs in InSAR processing. In this experiment, the InSAR DEM refined by registering and aligning to a reference DEM turned out better accuracy than only applying GCPs into InSAR processing.

SRTM 3 Arc Seconds (90 meter) DEM data is a good public accessible reference DEM to register and align a 15-30 meter (post spacing) InSAR DEM, since SRTM 3 Arc Seconds DEM data is available globally, except in polar regions.

REFERENCES

Ge, L., Li, X., Rizos, C. and Omura, M., 2004. GPS and GIS Assisted Radar Interferometry. *Photogrammetric Engineering & Remote Sensing*, 70(10): 1173–1177.

Gruen, A. and Akca, D., 2005. Least squares 3D surface and curve matching. *ISPRS Journal of Photogrammetry and Remote Sensing*, 59(3): 151-174.

Karkee, M., Kusanagi, M. and Steward, B.L., 2006. Fusion of Optical and InSAR DEMs Improving the Quality of Free Data, 2006 ASABE Annual International Meeting. American Society of Agricultural and Biological Engineers, Portland, Oregon.

LI, Z., Xu, Z., Cen, M. and Ding, X., 2001. Robust Surface Matching for Automated Detection of Local Deformations Using Least-Median-of-Squares Estimator. *Photogrammetric Engineering & Remote Sensing*, 67(11): 1283-1292.

Lin, Q., Vesecky, J.F. and Zebker, H.A., 1994. Comparison of elevation derived from INSAR data with DEM over large relief terrain. *International Journal of Remote Sensing*, 15(9): 1775 - 1790.

Lu, Z., Fielding, E., Patrick, M.R. and Trautwein, C.M., 2003. Estimating lava volume by precision combination of multiple baseline spaceborne and airborne interferometric synthetic aperture radar: the 1997 eruption of Okmok volcano, Alaska. *Geoscience and Remote Sensing, IEEE Transactions on*, 41(6): 1428-1436.

Mikhail, E.M., Bethel, J.S. and McGlone, J.C., 2001. *Introduction to Modern Photogrammetry*. John Wiley & Sons, Inc., New York, pp. 373-375.

Miliareisis, G.C. and Paraschou, C.V.E., 2005. Vertical accuracy of the SRTM DTED level 1 of Crete. *International Journal of Applied Earth Observation and Geoinformation*, 7(1): 49-59.

Orfanidis, S.J., 1996. *Optimum Signal Processing. An Introduction*. Prentice-Hall, Englewood Cliffs, NJ.

Pilgrim, L., 1996. Robust estimation applied to surface matching. *ISPRS Journal of Photogrammetry and Remote Sensing*, 51(5): 243-257.

Rufino, G., Moccia, A. and Esposito, S., 1996. DEM generation by means of ERS tandem data *Proceedings of the Fringe '96 Workshop ERS SAR*, Zurich, Switzerland.

Rufino, G., Moccia, A. and Esposito, S., 1998. DEM generation by means of ERS tandem data. *Geoscience and Remote Sensing, IEEE Transactions on*, 36(6): 1905-1912.

Sowter, A., Warren, M.A. and Bingley, R.M., 2006. The absolute positioning of spaceborne InSAR data using the integer ambiguity method. *Photogrammetric Record*, 21(113): 61-75.

Toutin, T., Hoja, D., Hoepfner, E., Remond, A. and King, C., 1998. GCPs selection from multi-source data over mountainous topography, *Geoscience and Remote Sensing Symposium Proceedings*, 1998. IGARSS '98. 1998 IEEE International, pp. 2339-2341 vol.5.

Zebker, H.A., Werner, C.L., Rosen, P.A. and Hensley, S., 1994. Accuracy of topographic maps derived from ERS-1 interferometric radar. *Geoscience and Remote Sensing, IEEE Transactions on*, 32(4): 823-836.

ACKNOWLEDGMENTS

ERS data were offered by the European Space Agency. Indiana high resolution DEM data were provided by [2005 Indiana Orthophotography (IndianaMap Framework Data www.indianamap.org)]. SRTM data were downloaded through USGS "The Seamless Data Distribution System (SDDS)"

